RESEARCH ARTICLE
PLANETARY SCIENCE

Earth and Planetary Physics
2: 398–405, 2018
doi: 10.26464/epp2018037

A new approach to study terrestrial yardang geomorphology based on high-resolution data acquired by unmanned aerial vehicles (UAVs): A showcase of whaleback yardangs in Qaidam Basin, NW China

Xiao Xiao, Jiang Wang, Jun Huang*, and Binlong Ye

Planetary Science Institute, School of Earth Sciences, China University of Geosciences, Wuhan 430074, China

Abstract: Yardangs are wind-eroded ridges usually observed in arid regions on Earth and other planets. Previous geomorphology studies of terrestrial yardang fields depended on satellite data and limited fieldwork. The geometry measurements of those yardangs based on satellite data are limited to the length, the width, and the spacing between the yardangs; elevations could not be studied due to the relatively low resolution of the satellite acquired elevation data, e.g. digital elevation models (DEMs). However, the elevation information (e.g. heights of the yardang surfaces) and related information (e.g. slope) of the yardangs are critical to understanding the characteristics and evolution of these aeolian features. Here we report a novel approach, using unmanned aerial vehicles (UAVs) to generate centimeter-resolution orthomosaics and DEMs for the study of whaleback yardangs in Qaidam Basin, NW China. The ultra-high-resolution data provide new insights into the geomorphology characteristics and evolution of the whaleback yardangs in Qaidam Basin. These centimeter-resolution datasets also have important potential in: (1) high accuracy estimation of erosion volume; (2) modeling in very fine scale of wind dynamics related to yardang formation; (3) detailed comparative planetary geomorphology study for Mars, Venus, and Titan.

Keywords: unmanned aerial vehicle (UAV); structure from motion; yardang; aeolian research; comparative planetary geology

Citation: Xiao X., Wang J., Huang J., and Ye B. L. (2018). A new approach to study terrestrial yardang geomorphology based on high-resolution data acquired by unmanned aerial vehicles (UAVs): A showcase of whaleback yardangs in Qaidam Basin, NW China. *Earth Planet. Phys.*, *2*(5), 398–405. http://doi.org/10.26464/epp2018037

1. Introduction

Yardangs are wind-eroded hills occurring in bedrocks and consolidated materials in arid regions (Hedin, 1907) on both Earth and Mars (Ward, 1979). They provide important geology and climate information. Numerous yardangs are identified in northwestern China, especially in Kumtagh Desert and Qaidam Basin (Fan XP, 1962; Halimov and Fezer, 1989; Dong ZB et al., 2012; Li JY et al., 2016; Xiao L et al., 2017; Anglés and Li YL, 2017; Wang J et al., 2018). Halimov and Fezer (1989) identified eight types of yardang in Qaidam Basin: mesa, saw-toothed crest, cone, pyramid, long ridge, hogback, whaleback, and low streamlined whaleback, and proposed a scenario for the evolution of the yardangs. Li JY et al. (2016) used satellite images available at Google Earth to study the distribution of yardangs in Qaidam Basin, and they measured length, width, spacing, and the orientation of mesa, whaleback, and long ridge yardangs. In addition, they adapted the model of yardang development proposed by Dong ZB et al. (2012), with its embryonic, adolescent, mature, and recession stages, and provided new observations in regional wind direction variations. Recently, Hu CQ et al. (2017) carried out a systematic geometric analysis of 16, 749 yardangs in Qaidam Basin, including aspect (length/width) ratio, spatial density, and spacing. Their results support the hypothesis that the different yardang geometries are mainly controlled by regional structures and rheology of the sedimentary rocks.

However, one major shortcoming of the previous geomorphology studies of yardangs in Qaidam Basin is the lack of topography of individual yardangs, due to the limitation of the satellite data's spatial resolution. In addition, the traditional field geometry measurements of the yardangs are time and effort consuming; they could reveal only very limited and unsatifactory information about the geomorphology.

In this study, we present a novel approach to the generation of ultra-high-resolution orthomosaics and digital elevation models (DEMs) for the whaleback yardangs in the Qaidam Basin (Figure 1). The centimeter-resolution data available to us provides unprecedented detailed information on the geomorphology characteristics of the whaleback yardangs and reveals new respects of their evolution. Such ultra-high-resolution data also have great potential in terrestrial aeolian research and detailed investigations of comparative planetary geomorphology.

Correspondence to: J. Huang, junhuang@cug.edu.cn
Received 13 AUG 2018; Accepted 25 SEP 2018.
Accepted article online 28 SEP 2018.

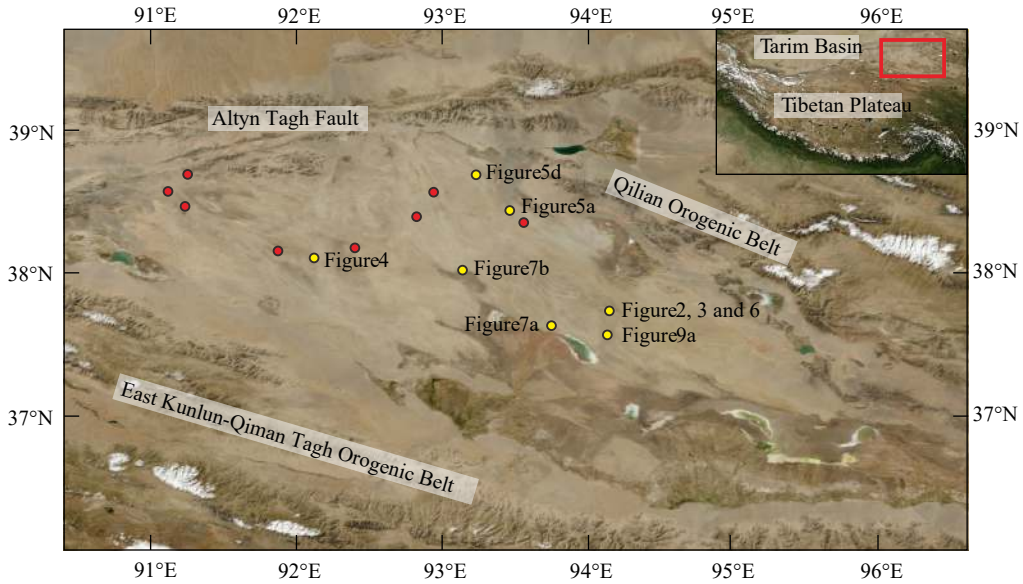

Figure 1. Locations of yardang fields in which we produced centimeter-resolution orthomosaics and DEMs. Yellow dots indicate locations of yardang fields presented in this study.

2. Methods

2.1 Hardware

During field investigations in the summer of 2017 we used a DJI Phantom 4 Pro drone to collect images in the yardang fields. The camera onboard the drone is equipped with a sensor of 1″ complementary metal-oxide-semiconductor (CMOS) with 20 million effective pixels and a lens of 84° field of view (FOV) and autofocus at 1 m – ∞. The images acquired are 5472 pixels × 3648 pixels, which means they are of 20-megapixel resolution. The average flight time of the drone with one battery is ~24 minutes. Additional drone specifications can be found at www.dji.com/phantom-4-pro/info#specs.

We used a combination of a Stonex S3 mobile station and a Stonex S6 base station (www.stonex.it) to measure the latitude, longitude, and elevation of the ground control points (GCPs) with an accuracy less than 1 cm. The GCPs markers were made of a compact disc (CD) glued at the center of an A3 size piece of red cardboard (297 mm × 420 mm). There were 10–20 GCPs distributed evenly in each measured region, allowing us to generate accurate orthomosaics and DEMs.

2.2 Software

We used Map Pilot for DJI (www.dronesmadeeasy.com/Articles.asp?ID=254) to plan the automatic routes for the drone to fly. The flight routes were designed with a forward overlap of 80% and a side overlap of 70%. The flight speed of the drone and the aperture of the camera onboard were adjusted by the software according to light conditions and wind speed during the flight.

After all the images were collected, we manually checked their quality and excluded ones of low quality. We imported the selected images into Agisoft PhotoScan Pro (http://www.agisoft.com/) to generate orthomosaics and DEMs of the yardang fields. The PhotoScan Pro software processed the images with the following procedures: (1) align images using embedded Global Positioning System (GPS) information; (2) manually select GCPs in the images (the A3-size red papers with CD glued on them) and input the latitudes, longitudes, and elevations of the GCPs recorded by the Stonex S3 mobile station; (3) optimize the alignment by applying corrections based on the lens parameters of the drone camera; (4) build a dense point cloud with structure from motion (SfM) algorithm and computer vision technology; (5) build a mesh from the dense cloud; (6) build a texture of the mesh; (7) build a DEM and orthomosaic of the study region.

The centimeter-resolution orthomosaics and DEMs were then imported into ArcMap for geomorphology analysis.

3. Results

3.1 Detailed Morphology Revealed by Centimeter Resolution Data

In Figure 2 we show a whaleback yardang field in Nanbaxian, its geomorphologic characteristics observed and analyzed with unprecedented centimeter resolution. We were able to generate high-resolution slope data (Figure 2c) from the DEM (Figure 2b) with a resolution of 2.8 cm/pixel. The variations of slope in the windward portions and leeward portions are consistent with the height profiles of the single whaleback yardang (Figures 3b and 3c). Interestingly, we have identified semi-solidified sand ripples around the yardang (Figure 2d). According to the extracted topographic profile (Figure 2e), most of the heights of these sand ripples range from ~10 to 30 cm.

Generally, these whaleback yardangs show a teardrop shape in plain view (Figure 2a), which consists of a larger "head" at the windward side and a tapered tail at the leeward side (Figure 3a). Contrary to traditional time-consuming and limited field measurements, use of the drone data allow us to extract centimeter resolution topographic profiles of a ~5 m high whaleback yardang

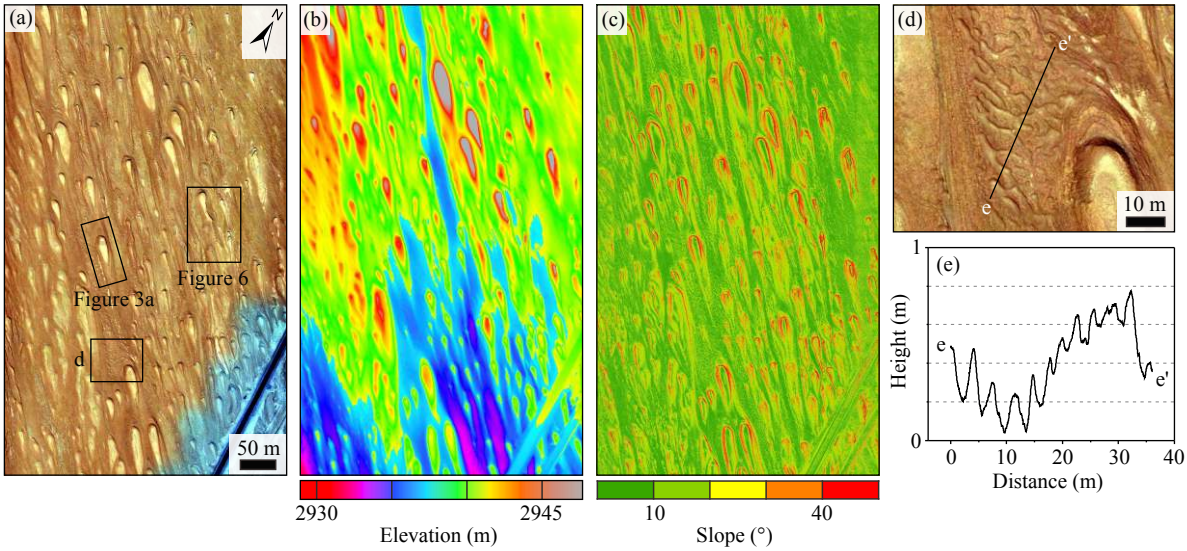

Figure 2. Whaleback yardang field in Nanbaxian. (a) The orthomosaic of the whaleback yardang field. The spatial resolution is 2.8 cm/pixel; (b) The DEM of the same whaleback yardang field in (a); (c) The slopes of the same whaleback yardang field in (a); (d) A subset of (a) showing that the yardang is surrounded by semi-solidified sand ripples. The black line indicates the location of the extracted height profile of the semi-solidified sand ripples; (e) The height profile of the semi-solidified sand ripples in (d); The height values are extracted from the DEM in (b).

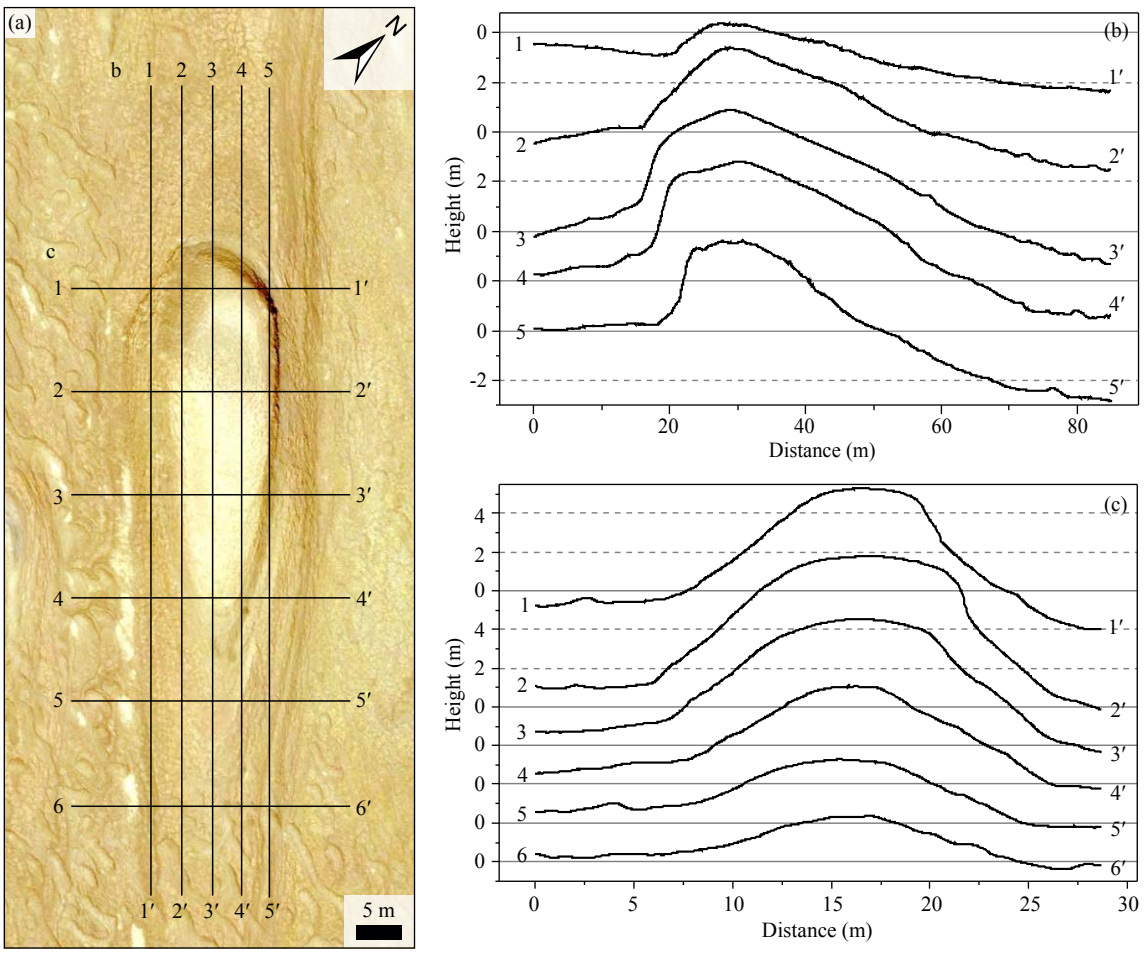

Figure 3. (a) The orthomosaic of the single whaleback yardang in Figure 2a. The black lines indicate the locations of the extracted height profiles of the yardang; (b) and (c) Height profiles of the yardang in (a).

(Figures 3b and 3c). These profiles show a steeper windward slope than the leeward portion and a steeper right side of the windward side.

We have identified moats around some of the whaleback yardangs. Figure 4 shows an example of a yardang with a moat. The depth of the moat is ~1 m, and its width ranges from ~2 to 4 m. The moats are difficult to identify even using the ultra-high-resolution orthomosaic presented in Figure 4 due to the limited amount of shadow in the scene. The centimeter resolution DEM provides a powerful tool to identify subtle local variations in elevation.

3.2 Evolution

3.2.1 Height increase of whaleback yardangs

We have identified whaleback yardangs that appear to have originated from mesa yardangs and long ridge yardangs, an evolution that has not been proposed by previous studies (e.g. Halimov and Fezer, 1989).

Mesa yardangs usually occur in horizontally bedded alluvial fans, initiated by erosion of ephemeral running water and modified by subsequent wind activity. Generally, mesa yardangs have irregular shapes with flat tops (Figure 5a). The ultra-high-resolution data reveal layers within the flanks of the mesa yardangs (Figure 5a), a feature that was not identified in the lower spatial resolution satellite images. Interestingly, we have identified different stages of whaleback yardangs clearly suggesting that they have evolved from the mesa yardangs (Figures 5b and 5c).

Long ridge yardangs usually develop in horizontal lacustrine mudstone strata (Fan XP, 1962), and are characterized by an elongated shape with a very large aspect ratio. We observe the detailed geomorphology of these long ridge yardangs, including their upwind and downwind shapes, and differences in their flanks (Figure 5d). Whaleback yardangs are observed to initiate from long ridge yardangs (Figure 5e), probably due to changes of wind direction (Hu CQ et al., 2017). The streamline shape of whaleback yardangs develope as they become more mature (Figure 5f).

3.2.2 Height reduction of whaleback yardangs

As a mature whaleback yardang continues to be eroded by wind

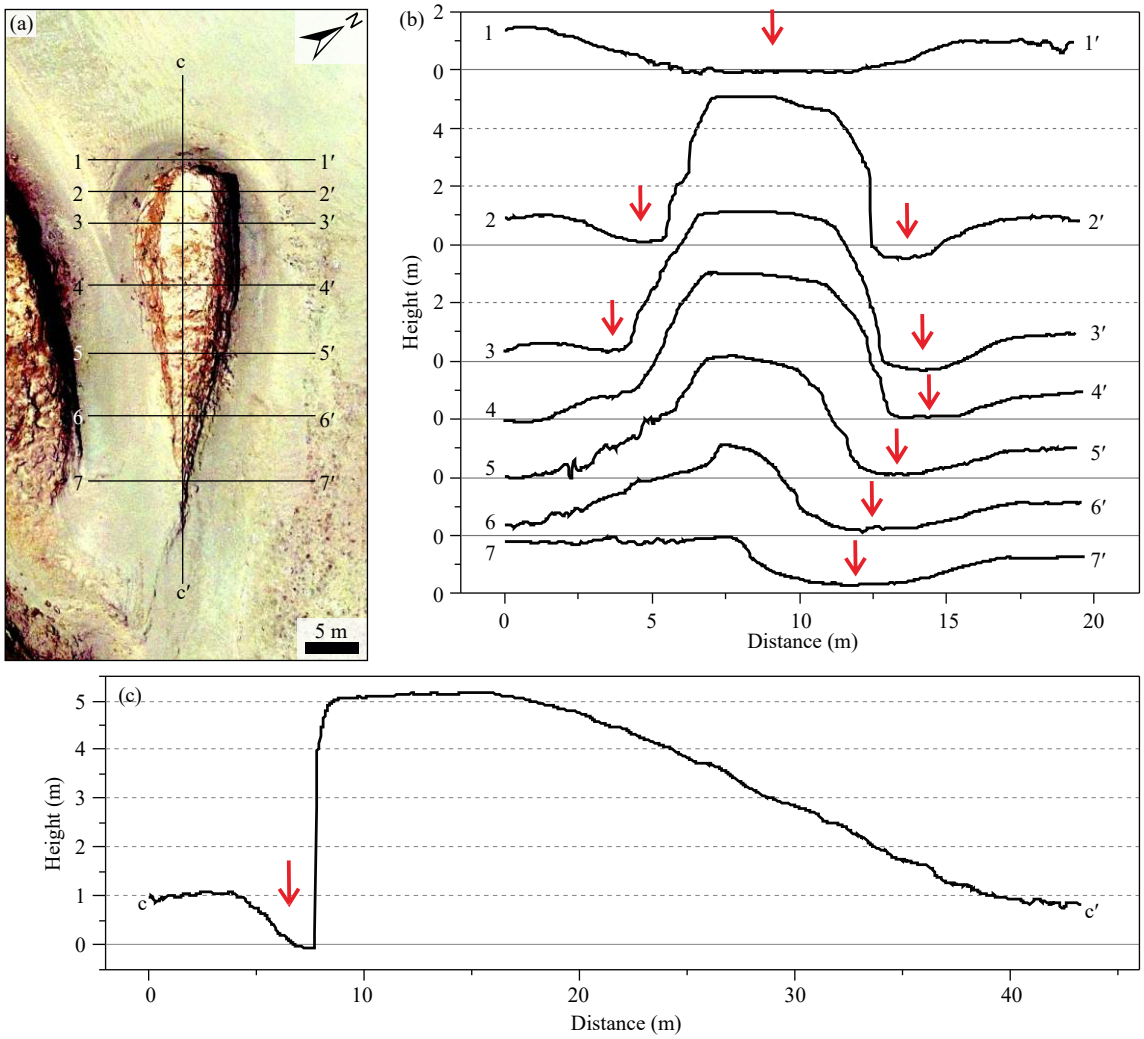

Figure 4. (a) A moat surrounding a whaleback yardang. The black lines indicate the locations of the extracted height profiles of the yardang. (b) and (c) Height profiles of the yardang in (a). The red arrows point to the local depression caused by the moat.

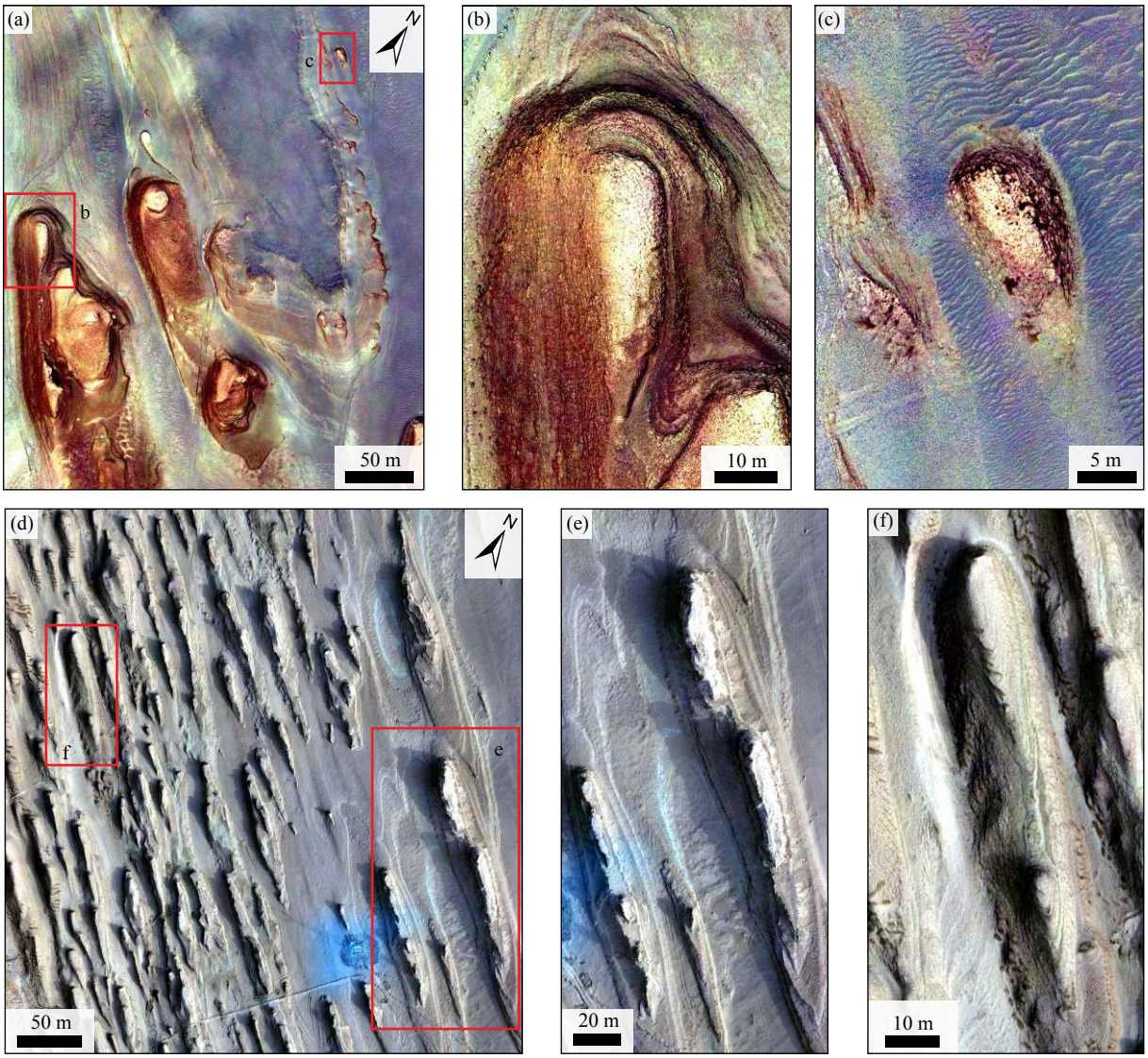

Figure 5. Examples of mesa yardang fields and long ridge yardang fields. (a) An orthomosaic of a mesa yardang field; (b) A whaleback yardang is initiated from one of the mesa yardangs. Layers of sediments can be identified; (c) A relatively mature whaleback originated from the mesa yardang nearby; (d) An orthomosaic of a long ridge yardang field; (e) Initial whaleback yardangs formed from long ridge yardangs; (f) Two relatively mature whaleback yardangs originated from a long ridge yardang.

abrasion and deflation, a portion of the yardang is likely to be destroyed (Figure 6). We can identify a relatively weak part of the previous yardang (Figure 6) in the Nanbaxian yardang field. When the erosion process continues, the height of the whaleback yardang is reduced. The result is a low streamlined whaleback yardang (Halimov and Fezer, 1989), and eventually it will disappear (Halimov and Fezer, 1989; Dong ZB et al., 2012).

In the Yiliping area is a group of water-related yardangs that are influenced by a seasonal lake. After being partially submerged, the yardangs are eroded by the water, forming steep cliffs (Figures 7a and 7b). Wind erosion continues above the surface of the water. The wind-eroded and water-eroded remnants are transported away by the water. Using the drone images and digital terrain model (DTM), we found four different possible watermarks, i.e., lines in Figures 7b and 7c. These watermarks may represent ancient water levels at different periods. Line 1 represents the possible highest water level, ~5 m above the present ground level (Figures 7d and 7e). Lines 2, 3, and 4 represent additional water levels at lower elevations. Line 4 may represent the largest visible extent of the yardang. We have measured the lengths and widths of the different period yardang parts, and find their aspect ratios to be 2.9:1, 3.2:1, 2.8:1, and 3.3:1 for the lines 1, 2, 3, and 4, respectively, which are consistent with previous data for whaleback yardangs under wind erosion (Li JY et al., 2016; Hu CQ, 2017; Wang J et al., 2018).

We selected 61 whaleback yardangs in relatively well-defined streamline shape in the Nanbaxian yardang field (Figure 2a), and measured their lengths, widths, and heights. Although the lengths and widths are both positively correlated with heights, the widths seem to have the better linear correlation (Figure 8). This plot indicates that the evolution process from whaleback yardangs to low streamlined whaleback yardangs maintains the

Figure 6. An example of whaleback yardangs eroded by wind.

relationships of lengths versus heights and widths versus heights. The streamline shapes are not only preserved in length and width during evolution (Ward, 1979), but also preserved in the third dimension, a feature first identified in this study.

4. Discussion

4.1 Accuracy Assessment of the DEMs

First, we evaluate the absolute accuracy of the DEMs. We generate the DEMs of test regions with a randomly selected subset of GCPs measured using the global navigation satellite system (GNSS) tools (a Stonex S3 mobile station and a Stonex S6 base station). Then we compare the calculated elevation extracted from the DEMs with the values of the rest of GCPs. The root-mean-square errors (RMSEs) between calculated and measured values are shown in Table 1.

Then we evaluate the accuracy of heights measured in the DEMs. The heights of whaleback yardangs can be up to 30 m, but most heights are between 2 and 8 m (Halimov and Fezer, 1989; Li JY et al., 2016; Hu CQ, 2017; Wang J et al., 2018). We selected a platform in Test Region 1 (Table 1) with a height of ~3.4 m. We measured the heights of 10 points on the platform edge to the ground by a Geomax ZT30R total station (http://www.geomax.cn/) whose ac-

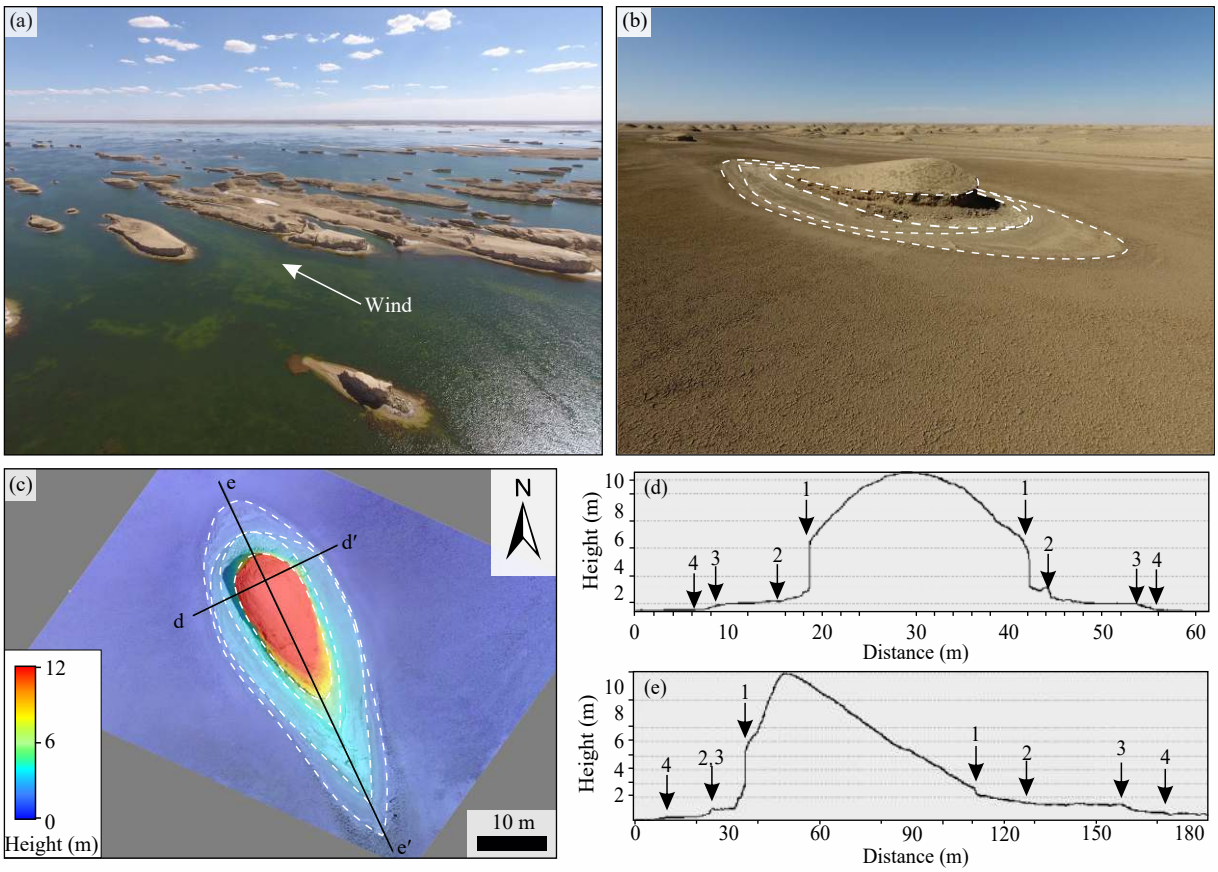

Figure 7. Water-influenced yardangs in the Yiliping area of the Qaidam Basin. (a) The water forms a seasonal salt lake; (b) A water eroded whaleback yardang. The white dashed lines represent the outlines of the yardangs at different water levels in (c), (d) and (e); (c) DTM superposed on the orthomosaic of the yardang in (b); (d) and (e) Height profiles of the yardang in (b) and (c). The black arrows mark the boundaries of the different stages, corresponding to the dashed white lines in (b) and (c).

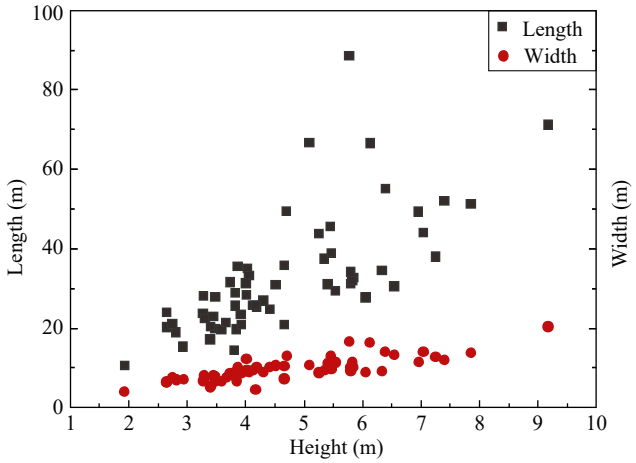

Figure 8. Measured lengths, widths, and heights of streamlined shape whaleback yardangs in Nanbaxian.

Table 1. Absolute accuracy of the test region DEMs

Test Region	Image Resolution (cm/pixel)	RMSE (cm)	
		Horizontal	Vertical
1	1.7	0.0	4.3
2	2.8	6.7	5.6
3	7.8	8.2	11.6
4	7.8	8.2	9.6

Table 2. Error analyses on the heights

	Calculated Height (cm)	Measured Height (cm)	Deviation (cm)	Relative Error (%)
1	337.1	337.4	–0.3	0.1
2	340.9	337.5	3.4	1.0
3	340.9	337.2	3.7	1.1
4	336.3	337.3	–1.0	0.3
5	336.1	337.3	–1.2	0.4
6	337.5	337.0	0.5	0.1
7	338.2	337.1	1.1	0.3
8	337.9	337.2	0.7	0.2
9	340.5	336.8	3.7	1.1
10	335.5	336.5	–1.0	0.3

curacy is ~2 mm. Then we compared the calculated heights (extracted from the DEM) of those 10 points to the measured values. The calculated heights, measured heights and their differences are shown in Table 2. Most of the relative errors are less than 1%.

Therefore, we expect the DEMs with all of the GCPs to have an accuracy close to single-pixel resolution (pixel size is of course dependent on the drone's flight altitude). The accuracy of DEMs built by use of Agisoft Photoscan Pro has been demonstrated to be suitable for detailed geomorphology analysis (Javernick et al., 2014; James et al., 2017).

4.2 Further Application of these Ultra-High-Resolution Yardang Data

We have generated and reported centimeter-resolution orthormosaics and DEMs for yardangs in Qaidam Basin for the first time. These unprecedented high-resolution data reveal characteristics of whaleback yardangs and some aspects of their evolution. We expect this dataset to play important roles in the following areas:

(1) Estimation of the volume of erosion. It is important to estimate the volume of sediment erosion over time; time can be determined by isotopes like ^{10}Be (Rohrmann et al., 2013). The high-resolution data presented in this study provides a novel way to estimate the volume of erosion of yardangs in an unprecedented accuracy. In addition, this dataset could provide a way to estimate the erosion rate within different time periods, instead of the average erosion rate estimated previously.

(2) Wind dynamic modeling. It has been very time and energy consuming to measure the geometry of yardangs in the field, and the measurements were able to reflect the geometries of the yardangs only in certain directions. Low resolution 3D models of yardangs were almost completely unable to model wind dynamics. The centimeter-resolution data presented in this study provide greatly improved 3D models for both the yardangs and yardang fields. Data sets of this sort have great potention to shed light onto past local wind characteristics.

(3) Comparative planetary study. Previous studies have shown that the yardangs in Qaidam Basin are closely analogous to yardangs on Mars (Xiao L et al., 2017; Anglés and Li YL, 2017; Wang J et al., 2018). However, the relatively low resolution of the terrestrial satellite data could not support a comprehensive comparative study of the yardangs on both planets. The current atmosphere pressure of Mars is about 1% of that on Earth. It should have taken a much longer time (maybe several orders of magnitude longer) for yardangs to form on Mars if the atmospheric pressure had been the same through the last 3 Ga (Carr and Head Ⅲ, 2010). However, the Mars yardang fields look very young. Therefore, the very high-resolution data presented in this study provide an opportunity for detailed geomorphology and paleo aerodynamic comparative study between the yardangs on Earth and those on Mars (Figure 9), Venus, and Titan.

5. Conclusion

In this paper, we present a useful approach for ultra-high-resolution remote sensing data acquisition. These centimeter-resolution datasets provide new insights into the geomorphological characteristics and evolution of whaleback yardangs in Qaidam Basin and have significant potential to contribute critical geomorphological information to aeolian research on Earth and other planets. The main conclusions are as follows:

(1) Semi-solidified sand ripples with heights of ~20 cm and moats with depths of ~1 m surround some whaleback yardangs.

(2) The whaleback yardangs may evolve from long ridge yardangs and from mesa yardangs. The heights of whaleback yardangs are reduced by wind abrasion and deflation, and they continue to evolve, finally becoming the low streamlined whalebacks.

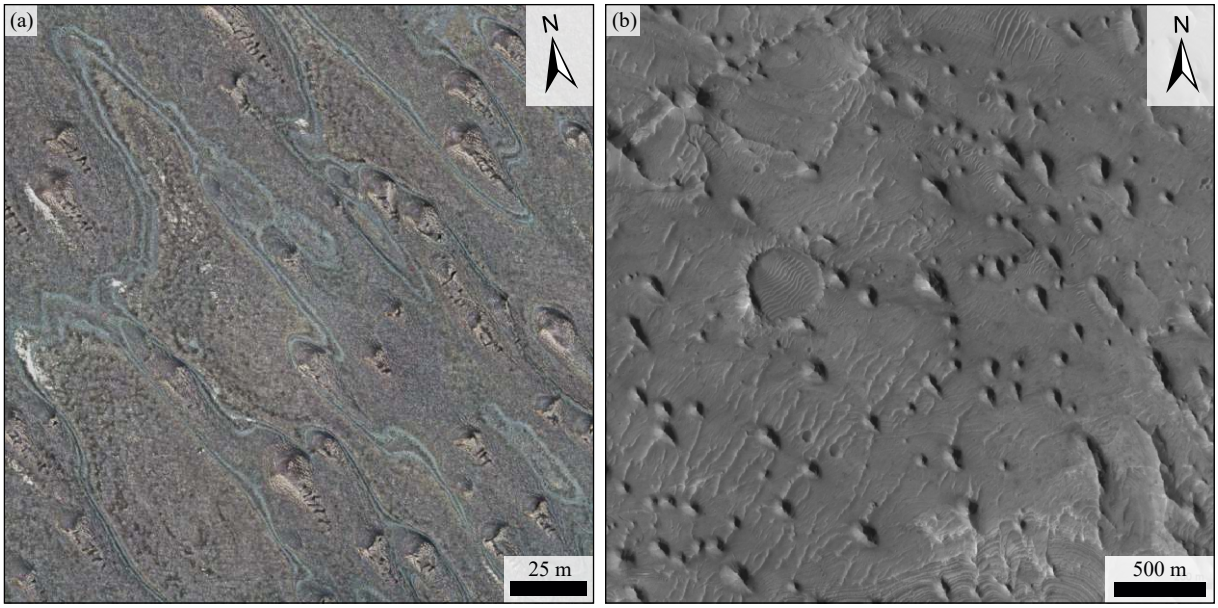

Figure 9. Whaleback yardangs on Earth and Mars. (a) Well developed streamlined whaleback yardangs in Nanbaxian in Qaidam Basin on Earth; (b) Similar whaleback yardangs (centered at –6.36°N, 283.20°E, a portion of the High Resolution Imaging Science Experiment (HiRISE) image: PSP_003474_1735_RED) on Mars.

(3) Several watermarks are found in the water-related yardangs, which may represent different ancient water levels. Their ratios of lengths and widths are similar to those of whalebacks under wind erosion.

(4) The evolution process from whaleback yardangs to low streamlined whaleback yardangs maintains their relationships between heights and widths and lengths; the relationship between heights and widths is especially strong.

(5) These formerly unattainable high-resolution data can be used in the estimation of the volume of erosion, wind dynamic modeling, and comparative planetary study.

Acknowledgments

Jun Huang was supported by the National Scientific Foundation of China (No. 41773061), the Fundamental Research Funds for the Central Universities, China University of Geosciences (Wuhan) (Nos. CUGL160402, CUG2017G02 and CUGYCJH18-01). We thank Dr. Rong Zou for the guide of GNSS operation. We appreciate the fieldwork assistance of Hansheng Liu, Jiawei Zhao, Ping Zhu, Limin Zhao, Xiaotong Huang, Kaidi Su, Xuelong Jiang, Yang Wu, Maomao Qu, and Ruixia La.

References

Anglés, A., and Li, Y. L. (2017). The western Qaidam Basin as a potential Martian environmental analogue: An overview. *J. Geophys. Res.: Planets*, *122*(5), 856–888. https://doi.org/10.1002/2017JE005293

Carr, M. H., and Head III, J. W. (2010). Geologic history of Mars. *Earth Planet. Sci. Lett.*, *294*(3-4), 185–203. https://doi.org/10.1016/j.epsl.2009.06.042

Dong, Z. B., Lv, P., Lu, J. F., Qian, G. Q., Zhang, Z. C., and Luo, W. Y. (2012). Geomorphology and origin of Yardangs in the Kumtagh Desert, Northwest China. *Geomorphology*, 139–154. https://doi.org/10.1016/j.geomorph.2011.10.012

Fan, X. P. (1962). Geomorphology of northwestern Qaidam Basin near Lenghu (in Chinese). *Acta Geogr. Sin.*, *28*(4), 275–289.

Halimov, M., and Fezer, F. (1989). Eight yardang types in Central-Asia. *Z. Geomorphol.*, *33*(2), 205–217.

Hedin, S. A. (1907). Scientific Results of A Journey in Central Asia, 1899-1902. In K. Boktryckeriet (Ed.), *Stockholm: Lithographic Institute of the General Staff of the Swedish Army*. P.A. Norstedt & söner.

Hu, C. Q., Chen, N. H., Kapp, P., Chen, J. Y., Xiao, A. C., and Zhao, Y. H. (2017). Yardang geometries in the Qaidam Basin and their controlling factors. *Geomorphology*, *299*, 142–151. https://doi.org/10.1016/j.geomorph.2017.09.029

Hu, C. Q. (2017). Yardang geometries and control factors in the Qaidam Basin based on multi-source remote sensing images [Master thesis] (in Chinese). Hangzhou: Zhejiang University.

James, M. R., Robson, S., d'Oleire-Oltmanns, S., and Niethammer, U. (2017). Optimising UAV topographic surveys processed with structure-from-motion: Ground control quality, quantity and bundle adjustment. *Geomorphology*, *280*, 51–66. https://doi.org/10.1016/j.geomorph.2016.11.021

Javernick, L., Brasington J., and Caruso B. (2014). Modeling the topography of shallow braided rivers using Structure-from-Motion photogrammetry. *Geomorphology*, *213*, 166–182. https://doi.org/10.1016/j.geomorph.2014.01.006

Li, J. Y., Dong, Z. B., Qian, G. Q., Zhang, Z. C., Luo, W. Y., Lu, J. F., and Wang, M. (2016). Yardangs in the Qaidam Basin, northwestern China: Distribution and morphology. *Aeolian Res.*, *20*, 89–99. https://doi.org/10.1016/j.aeolia.2015.11.002

Rohrmann, A., Heermance, R., Kapp, P., and Cai, F. L. (2013). Wind as the primary driver of erosion in the Qaidam Basin, China. *Earth Planet. Sci. Lett.*, *374*, 1–10. https://doi.org/10.1016/j.epsl.2013.03.011

Wang, J., Xiao, L., Reiss, D., Hiesinger, H., Huang, J., Xu, Y., Zhao, J. N., Xiao, Z. Y., and Komatsu, G. Geological features and evolution of Yardangs in the Qaidam Basin, Tibetan Plateau (NW China): a terrestrial analogue for Mars. *J. Geophys. Res.: Planets*. https://doi.org/10.1029/2018JE005719

Ward, A. W. (1979). Yardangs on mars: evidence of recent wind erosion. *J. Geophys. Res.: Solid Earth*, *84*(B14), 8147–8166. https://doi.org/10.1029/JB084iB14p08147

Xiao, L., Wang, J., Dang, Y. N., Chen, Z. Y., Huang, T., Zhao, J. N., Xu, Y., Huang, J., Xiao, Z. Y., and Komatsu, G. (2017). A new terrestrial analogue site for Mars research: The Qaidam Basin, Tibetan Plateau (NW China). *Earth-Sci. Rev.*, *164*, 84–101. https://doi.org/10.1016/j.earscirev.2016.11.003